Bulgarian Chemical Communications, Volume 50, Special issue H (pp. 34–39) 2018

Catalytic behaviour of nanostructured Ce-Mn oxide catalysts in ethyl acetate oxidation

R. N. Ivanova*, G. S. Issa, M. D. Dimitrov, T. S. Tsoncheva

Institute of Organic Chemistry with Centre of Phytochemistry, Bulgarian Academy of Sciences, 1113 Sofia, Bulgaria,

Received: January 31, 2018; Revised: March 06, 2018

Ce-Mn mixed oxide catalysts were prepared by co-precipitation method and used as catalysts for complete oxidation of ethyl acetate. The influence of Ce/Mn ratio was in the focus of the discussion in close relation with their catalytic activity. The obtained materials were characterised by different techniques, such as nitrogen physisorption, XRD, UV-Vis, and temperature-programmed reduction with hydrogen. A higher specific surface area favouring a higher catalytic activity as compared with pure CeO_2 and MnOx was established for all binary oxides. A strong effect of sample composition on dispersion and redox behaviour of the binary oxides was also found.

Key words: catalytic combustion, ethyl acetate, manganese oxide, ceria.

INTRODUCTION

Volatile organic compounds (VOCs) are one type of toxic pollutants to environment that are produced in variety of small and medium size industries. Among VOCs, ethyl acetate is a commonly used solvent, which can cause several environmental hazards. It can be completely oxidized to CO_2 by Pd, Pt supported catalyst at about 220–320 °C [1]. Some other papers [2–4] also reported attempts to eliminate low concentration of the ethyl acetate existing in gas steams. Recently, transition metal/metal oxides have been extensively studied for VOCs elimination as an alternative of the expensive noble based catalysts [5], but here the problem with the formation of products of partial oxidation, which are often very harmful for the human health, still exists. Among them, CeO_2-Mn_xO_y mixed oxides have been developed as environmentally friendly catalysts for the abatement of contaminants in both liquid and gas phases, such as oxidation of ammonia [6], pyridine [7], phenol [8], and acrylic acid [9]. Incorporation of manganese ions into ceria lattice greatly improved the oxygen storage capacity of cerium oxide as well as the oxygen mobility on the surface of the mixed oxides [10].

The present study deals with the effect of Ce/Mn ratio in CeO_2-Mn_xO_y mixed oxides on the catalytic behaviour of the latter in total oxidation of ethyl acetate. For this purpose, the catalysts were characterised by nitrogen physisorption, XRD, UV-Vis, and temperature-programmed reduction with hydrogen. A complicated relationship among sample structure, texture, redox properties, and catalytic activity was discussed.

EXPERIMENTAL

Materials

Manganese-cerium mono- and bi-component oxides of different composition were prepared by co-precipitation method. 1M NH_3 was added to an aqueous solution containing known amounts of $Mn(NO_3)_2.4H_2O$ and/or $Ce(NO_3)_2.6H_2O$ at room temperature until the pH of the solution was about pH=9.02. After 1 hour, the resulting precipitate was filtered, washed with distilled water, and dried at 373 K for 24 h. Metal oxide samples were obtained after calcination in air at 773 K for 5 h. The obtained catalysts were denoted as xCeyMn where x/y represents the Ce/Mn mol ratio.

Methods of characterisation

Powder X-ray diffraction patterns were collected on a Bruker D8 Advance diffractometer equipped with Cu Kα radiation and LynxEye detector. Nitrogen sorption measurements were recorded on a Quantachrome NOVA 1200e instrument at 77 K. Before physisorption measurements, the samples were outgassed overnight at 423 K under vacuum. UV-Vis spectra were recorded on a Jasco V-650 UV-Vis spectrophotometer equipped with a diffuse reflectance unit. TPR/TG (temperature-programmed reduction/thermogravimetric) analyses were performed on a Setaram TG92 instrument. Typically, 40 mg of the sample were placed in a microbalance crucible and heated in a flow of 50 vol.% H_2 in Ar

* To whom all correspondence should be sent
E-mail: *radostinaiv@abv.bg*

(100 cm^3min^{-1}) up to 773 K at 5 $Kmin^{-1}$ and a final hold-up of 1-h tests. The catalytic oxidation of ethyl acetate was carried out in a flow type reactor (0.030 g of catalyst) with a mixture of ethyl acetate and air (1.21 mol%) at WHSV of 100 h^{-1}. Before the catalytic experiments the samples were treated in argon at 373 K for 1 h. Experimental data were acquired under temperature-programmed regime in the range of 473–773 K. Gas chromatographic analyses were made on a HP 5890 apparatus using carbon-based calibration. Products distribution was calculated as CO_2 (S_{CO2}), acetaldehyde (S_{AA}), ethanol (S_{Et}), and acetic acid (S_{AcAc}) selectivity by the equation: $S_i = Y_i/X*100$, where S_i and Y_i were selectivity and yield of (i) product, respectively, and X was conversion. For a precise comparison, the conversion was normalised to unit surface area (SA = X/A, where X was the conversion at 650 K and A was the specific surface area of the sample).

RESULTS AND DISCUSSION

Nitrogen physisorption measurements were conducted in order to elucidate sample textural properties (Fig. 1, Table 1). All isotherms were of type IV according to IUPAC classification that is typical of mesoporous materials. They were characterised by well-pronounced step at about 0.6–0.8 relative pressure due to capillary condensation of nitrogen into the pores. The shape of the hysteresis loop indicated presence of uniform cage-like pores for 2Ce1Mn with average pore diameter about 5 nm. Slit-like pores of very wide size distribution was detected for all other metal oxide materials. The obtained binary oxides possessed a higher specific surface area as compared to the individual oxides and it increased almost linearly upon decrease of the manganese content in the samples. This could indicate formation of homogeneous metal oxide phase and further information about this was provided by XRD measurements of the samples (Fig. 2). The XRD pattern of pure manganese oxide contained intensive diffraction reflections at 2θ = 23.1°, 33.1°, 38.2°, 55.2°, and 65.9° due to well crystallised Mn_2O_3 phase (JCDS 41–1442) with relatively large crystallites. The latter provoked low surface area and pore volume for this material (Table 1). Additional weak reflections indicated presence of other crystalline phases, probably MnO_2, Mn_3O_4, which is in accordance with literature data [11,12]. Characteristic reflections at 2θ = 28.5°, 33.1°, 47.5°, and 56.4° in the XRD pattern of pure ceria matched crystal planes of (111), (200), (220), and (311) in cubic fluorite structure of CeO_2 (JCPDS 43-1002). Similar but broader reflections were also observed in the patterns of all bi-component samples. Here, no reflections of any manganese oxide phase could be detected. Thus, formation of ceria-manganese mixed oxide phase could be assumed [13]. Obviously, the incorporation of manganese in ceria rendered difficult the agglomeration of individual metal oxide phases, which provided an increase in dispersion (Fig. 2) and BET surface area (Table 1) of the composites.

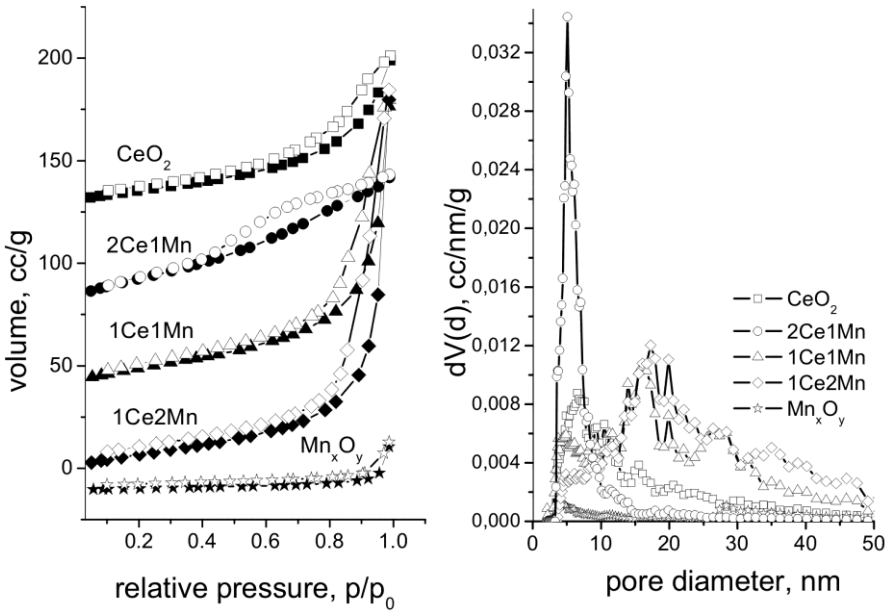

Fig. 1. Nitrogen physisorption isotherms (left) and pore size distribution (right) for pure and mixed metal oxide samples.

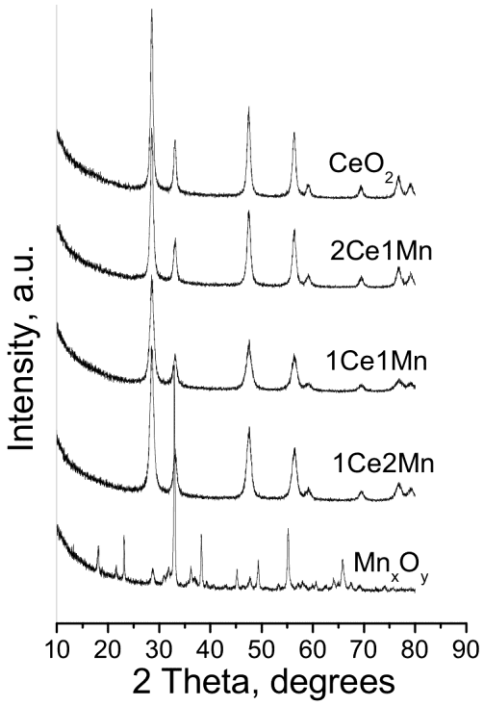

Fig. 2. XRD patterns of the studied samples.

Table 1. Texture parameters of the obtained oxides determined by low temperature nitrogen physisorption (specific surface area S_{BET}; total pore volume Vt, and specific activity SA)

Sample	S_{BET}, m^2g^{-1}	V_t, cm^3g^{-1}	Conversion, 610 K	SA, 610 K
CeO_2	47.5	0.12	60	1.26
2Ce1Mn	82.2	0.10	81	0.98
1Ce1Mn	66.9	0.21	90	1.35
1Ce2Mn	57.6	0.26	84	1.46
Mn_xO_y	7.4	0.025	88	11.89

UV-Vis spectra were recorded to characterise precisely the oxidation state of metal oxide species (Fig. 3). The spectrum of manganese oxide represented a continuous absorption feature, which is due to variations in manganese oxidation state (Mn^{2+}, Mn^{3+}, and Mn^{4+}). The absorption band at about 250 nm was attributed to a charge transfer between O^{2-} and Mn^{2+}. Absorption at approximately 300 nm was related to Mn^{4+} and the continuous absorption above 300 nm is assigned to $O^{2-} \rightarrow Mn^{3+}$ charge transfer and d-d transition for d4 electronic configuration in octahedral field [14]. Simultaneous presence of MnO_2 and Mn_2O_3 after precursor decom-position in air at a temperature above 623 K was also reported by Milella *et al*. [15]. The spectrum of pure ceria represented two maxima at about 250 and 305 nm that could be attributed to $Ce^{4+} \leftarrow O^{2-}$ charge transfer (CT) and interband transitions, respectively [16]. The latter peak was also assigned to lattice defects. The former band was broad and it may be superposed together with the band of $Ce^{3+} \leftarrow O^{2-}$ charge transfer transition. The observed features in the spectra of bi-component materials could not be simply assigned to superposition of the spectra of single oxides. These results confirmed changes in the environment and/or oxidation state of metal ions probably due to formation of solid solution.

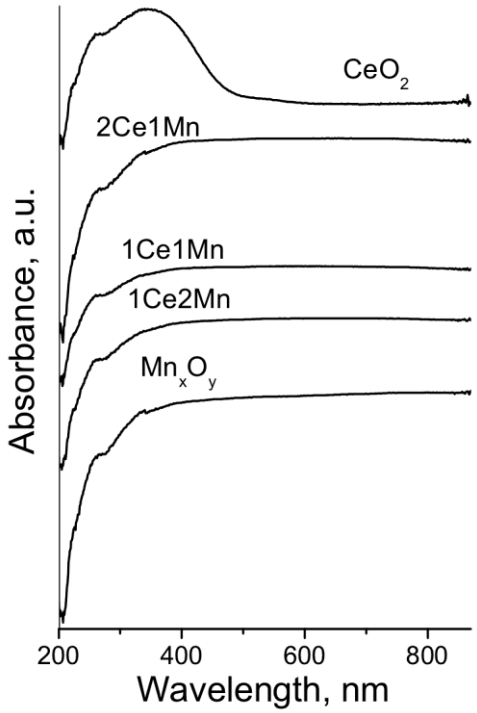

Fig. 3. UV-Vis spectra of the studied samples.

Further information for about the redox properties of the studied materials was obtained by temperature-programmed reduction (TPR) with hydrogen (Fig. 4). The reduction effects over 570 K for pure CeO_2 were generally assigned to surface Ce^{4+} to Ce^{3+} transition [17]. The reduction degree was about 4% (Table 2).

The DTG-TPR profiles of Mn_xO_y sample (Fig. 4, right) consisted of two reduction effects for low and high temperature regions. They are generally assigned to step-wise reduction of MnO_2 (or Mn_2O_3) to Mn_3O_4 and further reduction of Mn_3O_4 to MnO, respectively [18, 19]. A decrease in the overall reduction degree upon ceria increase in the binary materials (Table 2) indicated stabilised Mn-O bonds near Ce^{4+} ions. However, here the reduction transformations were broader and shifted to lower initial temperatures. This observation, combined with an increase in the ratio of the low temperature to high temperature reduction effects could be an indication for the increased Mn^{4+} content at the expense of manganese ions of lower oxidation state in the samples. In accordance with the XRD and UV-Vis data, this could be provoked by stabilisation of Mn^{4+} ions *via* incorporation in the ceria lattice. Changes

in the reduction degree (Table 2) showed that the portion of Mn^{4+} ions shared with Ce^{4+} could be controlled by the Ce/Mn ratio and it seemed to be the highest for 1Ce2Mn (Table 2).

Fig. 5 gives temperature dependencies of catalytic activity in ethyl acetate (EA) oxidation for all studied samples. CO_2, ethanol (Et), acetaldehyde (AA), and acetic acid (AcAc) in different proportion with temperature rise were registered. For all samples, ethyl acetate oxidation was initiated over 500 K and an 80–100% conversion was achieved above 650 K combined with high CO_2 selectivity. Between the pure oxides, manganese oxide exhibited a higher catalytic activity. According to their catalytic activity, the bi-component mixed oxide materials are arranged in the following order: 1Ce1Mn > 2Ce1Mn ≈ 1Ce2Mn. All of them provided a higher catalytic activity than the mono-component samples, which could be due to the existence of a synergistic effect between the ceria and manganese oxide species and/or owing to higher dispersion and specific surface area.

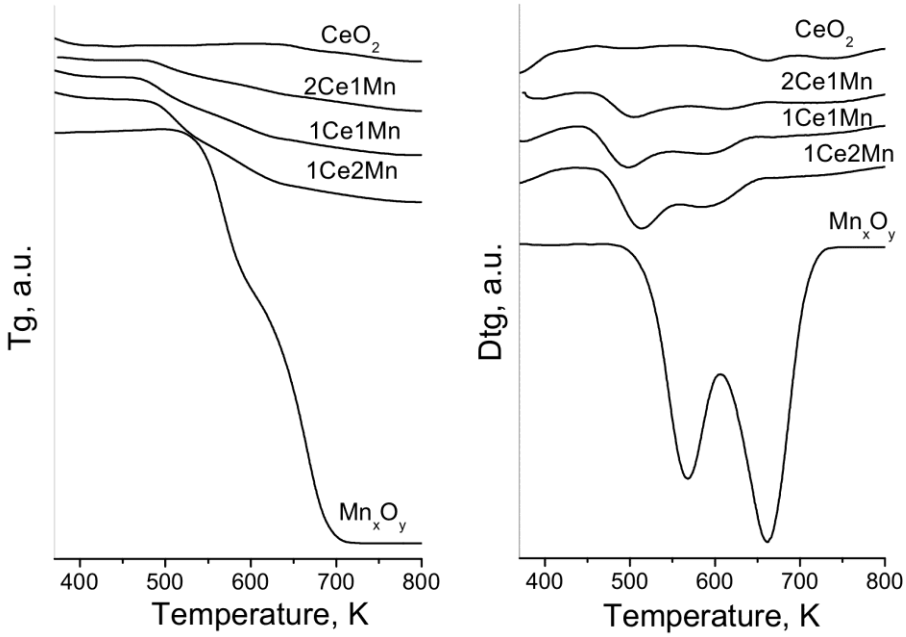

Fig. 4. TG (left) and DTG (right) data on the samples.

Table 2. TPR data for all samples (T_{ini}-initial reduction temperature, T_{max} - maximum of the reduction peak $Mn^{3+}\rightarrow Mn^{2+}$; $Mn^{4+}\rightarrow Mn^{2+}$)

Sample	T_{ini}. K	T_{max} K	Weight loss, theoretical, mg	Weight loss, experimental, mg	Reduction degree, %
Mn_xO_y	482	565, 662	4.05 (Mn_2O_3)	4.73	116
			2.79 (Mn_3O_4)		169
			9.01 (MnO_2) (to Mn^{2+})		52
1Ce2Mn	458	515, 596	0.94 (Mn_2O_3)	1.12	119
			0.68 (Mn_3O_4)		164
			1.62 (MnO_2)		69
1Ce1Mn	445	497, 592	0.91 (Mn_2O_3)	0.86	95
			0.8 (Mn_3O_4)		107
			2.08 (MnO_2)		41
2Ce1Mn	460	503, 620	0.90 (Mn_2O_3)	0.58	64
			0.46 (Mn_3O_4)		126
			1.58 (MnO_2)		37
CeO_2	577	660, 738	3.72 (Ce^{4+} to Ce^{3+})	0.14	4

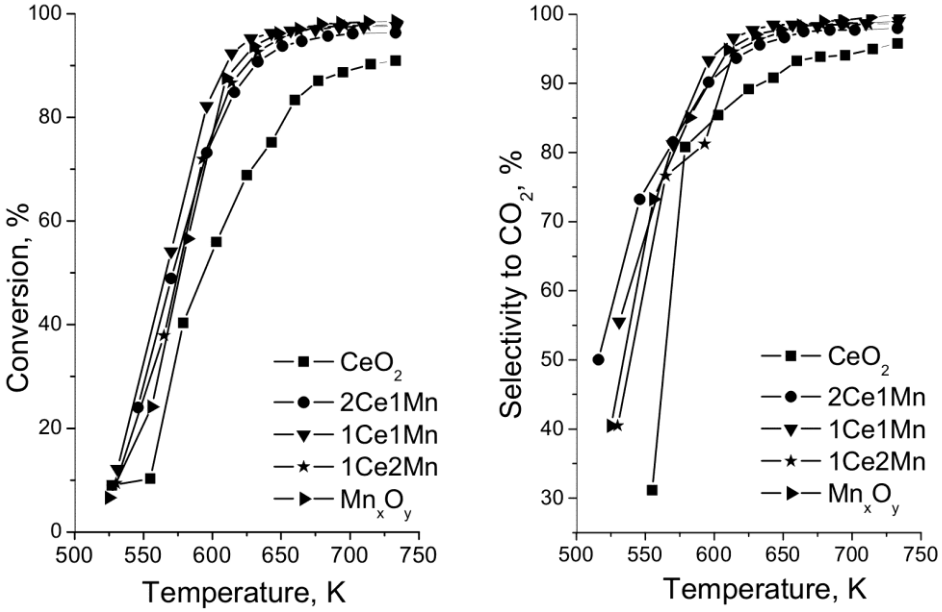

Fig. 5. Temperature dependence of ethyl acetate total oxidation (left) and selectivity to CO_2 (right) for the studied samples.

Over 80% selectivity to CO_2 for all samples was detected (Table 3). A slight tendency to form by-products (acetaldehyde and ethanol) with the the binary oxides was observed. Specific catalytic activity (SA) per unit BET surface area was calculated as a measure of conversion to elucidate the impact of textural parameters on sample catalytic behaviour (Table 1). Note an extremely high SA value for pure Mn_xO_y, which clearly indicates the decisive role of the oxidation state of the manganese ions in the samples. The SA values for all binary materials were much lower than expected if the samples were simple mechanical mixtures of individual oxides.

Table 3. Results from the catalytic tests: selectivity to acetaldehyde (S_{AA}), ethanol (S_{Et}), acetic acid (S_{AcAc}), and CO_2 (S_{CO2}) at 50% conversion of ethyl acetate.

Sample	Conversion, %	S_{AA} %	S_{Et} %	S_{AcAc} %	S_{CO2} %
Mn_xO_y	50	12	2		86
1Ce2Mn	50	13	5	1	81
1Ce1Mn	50	17	1		82
2Ce1Mn	50	11	6	1	82
CeO_2	50	7	6	1	86

Thus, the enhanced catalytic activity of the binary materials could mainly be related to both increased dispersion and specific surface area. In accordance with the TPR data, the decrease in SA for the binary materials could be due to stabilisation of the lattice oxygen ions *via* formation of shared Mn-O-Ce bonds, which renders difficult the EA oxidation *via* Mars-van-Krevelen mechanism [20]. The TPR data also revealed that the increase in SA with the increase of Mn content in the binary oxides could be due to stabilised Mn^{4+} ions *via* their incorporation in the ceria lattice.

CONCLUSIONS

Binary manganese-cerium oxides exhibited higher dispersion and higher specific surface area, but suppressed reduction ability as compared to the individual oxides. Catalytic activity and selectivity in ethyl acetate combustion could be regulated by variation of the Ce/Mn ratio in the samples. Formation of shared Ce-O-Mn bonds and an increase of the Mn content facilitated the formation of more active Mn^{4+} -Mn^{3+} pairs in ethyl acetate oxidation.

Acknowledgement: *Financial support by 'Program for career development of young scientists', BAS (project DFNP 17-65/26.07.2017) is gratefully acknowledged.*

REFERENCES

1. Y. Yang, X. Xu, K. Suna, *J. Hazard. Mater. B*, **139**, 140 (2007).
2. P. Papaefthimiou, T. Ioannides, X. Verykios, *Appl. Thermal Eng*., **18**, 1005 (1998).
3. P. Papaefthimiou, T. Ioannides, X. Verykios, *Appl. Catal. B.*, **15**, 75 (1998).
4. X. Wang, M. Landau, H. Rotter, *J. Catal.* **222**, 565 (2004).
5. P. Lin, M. Skoglundh, L. Lowendahl, *Appl. Catal. B*, **6**, 237 (1995).
6. Z. Ding, L. Wade, E. Gloyna, *Ind. Eng. Chem. Res.*, **37**, 1707 (1998).

7. S. Aki, M. Abraham, *Ind. Eng. Chem. Res.*, **38**, 358 (1999).
8. H. Chen, A. Sayari, A. Adnot, F. Larachi, *Appl. Catal. B*, **32**, 195 (2001).
9. A. Silva, R. Marques, R. Quinta-Ferreira, *Appl. Catal. B*, **47**, 269 (2004).
10. X.Tang, Y. Li, X. Huang, Y. Xu, H. Zhu, J. Wang, W. Shen, *Appl. Catal. B*, **62**, 265 (2006).
11. S. Todorova, A. Naydenov, H. Kolev, K. Tenchev, G. Ivanov, G. Kadinov, *J. Mater. Sci.*, **46**, 7152 (2011).
12. S. Kanungo, *J. Catal.*, **58**, 419 (1979).
13. M. Machida, M. Uto, D. Kurogi, T. Kijima, *Chem. Mater.*, **12**, 3158 (2000).
14. Y. Lin, S. Ming, Y. Jian, Y. Qian, H. Zhifeng, L. Chaosheng, *Chin. J. Catal.*, **29**, 1127 (2008).
15. F. Milella, J. Gallardo-Amores, M. Baldic, G. Busca, *J. Mater. Chem.*, **8**, 2525 (1998).
16. A. Kambolis, H. Matralis, A. Trovarelli, C. Papadopoulou, *Appl. Catal. A*, **377,** 16 (2010).
17. L. Shi, W. Chu, F. Qu, J. Hu, M. Li, *J. Rare Earths*, **26**, 836 (2008).
18. Y. Du, Q. Meng, J. Wanga, J. Yan, H. Fan, Y. Liu, H. Dai, *Micropor. Mesopor. Mater*. **162**, 199 (2012).
19. D. Delimaris, T. Ioannides, *Appl. Catal. B*, **84**, 303 (2008).
20. P. Larsson, A. Andersson, *Appl. Catal. B*, **24**, 175 (2000).

КАТАЛИТИЧНИ СВОЙСТВА НА НАНОСТРУКТУРИРАНИ Ce-Mn ОКСИДНИ КАТАЛИЗАТОРИ ЗА ОКИСЛЕНИЕ НА ЕТИЛАЦЕТАТ

Р. Н. Иванова*, Г. С. Исса, М. Д. Димитров, Т. С. Цончева

Институт по органична химия с Център по фитохимия, БАН, 1113 София, България

Постъпила на 31 януари 2018 г.; Преработена на 6 март 2018 г.

(Резюме)

За настоящото изследване бяха получени Ce-Mn смесени оксидни катализатори за изгаряне на етилацетат чрез метод на съутаяване. Специално внимание бе обърнато на влиянието на съотношението на Ce/Mn, което е в тясна връзка с каталитичната им активност. Получените материали бяха характеризирани с помощта на различни методи, сред които азотна физисорбция, прахова рентгенова дифракция, УВ-видима спектроскопия и температурно-програмирана редукция с водород. Резултатите от физикохимичните изследвания показаха, че бинарните материали притежават по-висока специфична повърхност, което благоприятства по-високата каталитична активност в сравнение с еднокомпонентните оксиди. Беше установен значителен ефект на състава на образците върху тяхната дисперсност и редокси свойства.